Aalto University

Aaltodoc

OPEN ACCESS

This is an electronic reprint of the original article.
This reprint may differ from the original in pagination and typographic detail.

Author(s):   Puska, M. J. & Nieminen, Risto M.

Title: Positron and electron energy levels in rare-gas solids

Year: 1992

Version: Final published version

Positron and electron energy levels in rare-gas solids

M. J. Puska and R. M. Nieminen

Laboratory of Physics, Helsinki University of Technology, 02150 Espoo, Finland

(Received 29 January 1992)

The positron and electron band structures are calculated for the rare-gas solids Ne, Ar, Kr, and Xe on the basis of density-functional theory. The effects due to different approximations for the positron correlation and electron exchange-correlation potential are studied. The positron band structures obtained are compared with the measured band gaps in the $\langle 111 \rangle$ direction and with the measured positron work functions. A semiempirical positron correlation potential is presented.

I. INTRODUCTION

In the field of slow-positron beams,[1] rare-gas solids have attracted interest as possible efficient positron moderators[2,3] or sources of thermalized positronium atoms.[4] From the theoretical point of view, the rare-gas solids are challenging as test cases for different descriptions of exchange and correlation effects. The most popular method, i.e., the local-density approximation (LDA), fails to give the correct electron band gaps and work functions for insulators and semiconductors.[5] In this paper we report systematic theoretical studies of positron band structure and chemical potential in rare-gas solids. Among other things we show that LDA for the positron correlation potential cannot describe the positron energetics in rare-gas solids, and present a form for the correlation potential. The calculated positron band gaps are in excellent agreement with experiments.[2,6]

Energetic positrons from a radioactive source introduced into a rare-gas solid lose their energy rapidly in ionization and electron-hole pair-creation processes. When the positron kinetic energy has decreased to the value corresponding to the electron energy gap between the valence and conduction bands these processes become impossible. Thereafter, processes which lead to the formation of an exciton or a positronium atom are possible when the positron energy is a few eV below the electron energy gap. Finally, only phonon creation processes are able to receive energy from the positron. Because in the rare-gas solids the band gaps are large, i.e., from 21.7 eV (Ne) to 9.3 eV (Xe), and the phonon energies are much smaller, of the order of meV's, positrons remain "hot" for a relatively long time period. Since the diffusion length for these hot positrons is large, a substantial fraction of them reaches the solid surface and are emitted as slow positrons into vacuum. For example, Mills and Gullikson[3] found that the solid Ne moderator emits slow positrons up to 0.70% of the positron flux incident from the radioactive source. This efficiency is about twice as large as that for the best conventional metal moderators.

II. THEORY

The energy thresholds for positronium, exciton, and electron-hole pair formations discussed in the Introduc-

tion are clearly seen in experiments in which a monoenergetic positron beam with an energy around the electron energy band gap hits the solid rare-gas target and the reemitted positron yield is measured.[2,3] The measured positron yield also shows peaks corresponding to the Bragg scattering of the positrons.[2,6] This means that the positrons cannot penetrate into the sample if their energy is within the forbidden energy gaps of the *positron* band structure.

The first-order Bragg peaks give experimental information about the positron band structure which can be compared with the theoretical results presented below. First, for a positron beam perpendicular to the surface the energy gaps are in the **k** space in the $\langle 111 \rangle$ direction at the L point of the Brillouin zone because the rare-gas solids grow along the $\langle 111 \rangle$ direction.[7] According to Gullikson, Mills, and McRae,[6] the first-order Bragg peak has a "top-hat" shape and its width corresponds to the first positron energy gap, E_g^+, at the L point. The position of the center of the peak, E_{Bragg}^+, is also determined. Assuming that the positron band mass is equal to the free-positron mass the position of the bottom of the positron bands is (atomic units with $\hbar = e = m_e = 1$ are used in this paper)

$$V_0^+ = E_{\text{Bragg}}^+ - k_L^2/2 . \tag{1}$$

Above, k_L is the positron **k** vector at the L point. The negative of V_0^+ is identified as the positron work function ϕ^+. Gullikson, Mills, and McRae[6] determined the parameters E_g^+ and E_{Bragg}^+ for the solid Ne, Ar, Kr, and Xe.

The electron structures of the rare-gas solids are calculated in this work using the LDA of the density-functional theory. In the LDA the effective potential for the electrons has the form

$$v_{\text{eff}}^-(\mathbf{r}) = v_{\text{Coul}}(\mathbf{r}) + v_{\text{xc}}(n(\mathbf{r})) , \tag{2}$$

where $v_{\text{Coul}}(\mathbf{r})$ is the Coulomb potential due to the nuclei and electron charge density $n(\mathbf{r})$. v_{xc} is the LDA exchange-correlation potential,[8,9] which depends on the electron density at the given point $\mathbf{r}$, only. The corresponding electron eigenfunctions and eigenenergies are solved scalar relativistically (no spin-orbit splitting) by using the self-consistent linear muffin-tin-orbital atomic-sphere approximation (LMTO-ASA) method with the

so-called combined correction.[10]

In the LDA for positron states the potential is constructed as

$$v_{\text{eff}}^{+}(\mathbf{r}) = -v_{\text{Coul}}(\mathbf{r}) + v_{\text{corr}}(n(\mathbf{r})) , \qquad (3)$$

where v_{corr} is the correlation potential describing the energy lowering due to the electron pileup near the positron. It is determined by many-body calculations for a delocalized positron in a homogeneous electron gas.[11] The positron band structure is also calculated by the LMTO-ASA method. No self-consistency iterations are needed for the delocalized positron states. The LDA method has been applied for positron and electron energetics in metals and semiconductors.[12,13] In the case of semiconductors the correlation potential is slightly modified to account for the imperfect screening.[14]

The LDA for the correlation potential breaks down in cases where the screening cloud is not isotropic around the positron. This happens, e.g., for positrons outside solid surfaces and inside large voids because the screening cloud is left behind in the solid and an imagelike potential is formed. The situation is analogous in insulators such as rare-gas solids where the screening or the correlation effects consist of the polarization of the atomic electron structures. At large distances the attractive positron-atom polarization interaction decays as $-\frac{1}{2}\alpha/r^4$, where α is the polarizability of the atom. At small distances the correlation potential remains finite, but has no simple form. In practice, the actual form of the correlation potential at very small distances is not important because the repulsive Coulomb potential dominates in this region. In this work we have used two models for the correlation potential in rare-gas solids.

Schrader[15] suggested a simple model for the positron-atom correlation potential. The potential is set to a constant at distances smaller than a certain cutoff radius r_0, i.e.,

$$V_{\text{corr}}(r) = \begin{cases} -\frac{1}{2}\alpha/r^4 & \text{when } r \geq r_0 \\ -\frac{1}{2}\alpha/r_0^4 & \text{when } r < r_0 . \end{cases} \qquad (4)$$

Schrader determined the cutoff radius r_0 by fitting the calculated positron scattering lengths for H and He atoms and the calculated positronium affinity of H to the measured values. For the other atoms he presented an interpolation form based on the dependence on the ionization potential. We have applied Schrader's potential for the rare-gas solids with fcc lattice structures by calculating the spherical average of the superposition of atomic contributions. Thirty nearest-neighbor shells are used in the superposition. The contribution of the rest of the atoms is taken into account by replacing the summation by integration which gives a constant shift of $-8\pi\alpha/a^3R_M$. Here a is the fcc lattice constant and R_M is the lower limit of the integration. The polarizabilities α and cutoff radii r_0 used in this work are given in Schrader's paper.[15]

As will be discussed below, Schrader's model applied in the positron band-structure calculations does not repro-

TABLE I. Parameters used in calculations and results for the positron band gap E_g^+. a and α are the fcc lattice constant (Ref. 18) and the atomic polarizability (Ref. 19), respectively. The band gaps obtained using the present correlation potential model of Eq. (5) (PW) are compared with the measured ones (expt) (Ref. 6).

Host	a (a.u.)	α (a.u.)	E_g^+(PW) (eV)	E_g^+(expt) (eV)
Ne	8.37	2.663	1.56	1.60±0.1
Ar	9.93	11.06	1.52	1.50±0.05
Kr	10.81	16.74	1.27	1.30±0.05
Xe	11.71	27.29	1.06	1.05±0.05

duce quantitatively the experimental results of Gullikson, Mills, and McRae.[6] However, the model gives quite well the trend for the width of the band gap E_g^+. This suggests that one could determine r_0 by fitting to the measured values of the band gap. Schrader's potential has, however, the undesired feature of a discontinuous derivative at r_0. Therefore, in order to make the correlation potential smooth, we choose the following form first used by Abarenkov and Antonova[16] for polarization effects in alkali halides:

$$V_{\text{corr}}(r) = -\frac{1}{2}\alpha/(r^2+r_1^2)^2 . \qquad (5)$$

The polarizabilities α (see Table I) are the same as in Schrader's construction. The results (see below) turn out to be insensitive to the cutoff parameter r_1. With a single value of r_1, we obtain excellent agreement with experiment.

III. RESULTS AND DISCUSSION

The total positron potentials obtained in the different models are shown for Ar in Fig. 1. The potentials are spherical averages around an atom in the fcc lattice. The pure Coulomb potential (COUL) and the LDA potential give the upper and lower limits, respectively, for the more sophisticated semiempirical models. At large dis-
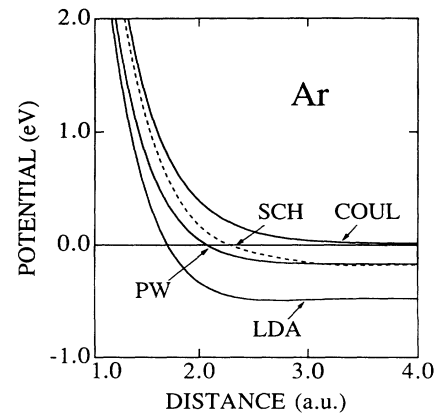

FIG. 1. Spherically averaged total positron potentials around an atom in solid Ar in different models for the positron correlation potential.

tances the present model potential (PW) [Eq. (5)] is slight-
ly above Schrader's potential (SCH), whereas at smaller
distances it is close to the LDA potential.

The electron and positron band structures obtained for
solid Ar are shown in Figs. 2 and 3, respectively. The
correlation potential for the positron states is treated in
the model introduced in this work [Eq. (5)]. The
valence-electron band, i.e., the $3p$ band, shows only a
small energy dispersion whereas the bottom of conduc-
tion bands is clearly free-electron-like. The band gap be-
tween the valence and conduction bands is is about 40%
narrower than the experimental band gap. The same
trend is true also for the other rare-gas solids as can be
seen from Table II. The results for the band gaps are in
accord with previous LDA calculations[17] and the nar-
rowness is a well-known deficit of the LDA.[5]

As can be seen from Fig. 3, the positron bands are
close to free-particle bands, but there are gaps at the
Brillouin-zone boundary. The center of the first band gap
at the L point, E^+_{Bragg}, is within 0.05 eV at the energy pre-
dicted by the free-particle model with positron band mass
equal to the free-positron mass. This justifies the use of
Eq. (1) in the determination of the position of the bottom
of positron bands and thereby also the determination of
positron work function.

The positron band gaps calculated for the rare-gas
solids using the different positron correlation potential
models as well as omitting it altogether (pure Coulomb)
are shown in Fig. 4. The use of the pure Coulomb poten-
tial gives much too large band gaps. Gullikson, Mills,
and McRae[6] found that the corresponding Fourier com-
ponent of the Coulomb potential used in a nearly-free-
electron model gives even larger band gaps. According
to Fig. 4, the pure Coulomb potential leads to a max-
imum at Ar, which is not seen in the experimental data.
The inclusion of the correlation makes the band gaps nar-
rower. The LDA exaggerates the correlation effects and
the wrong trend between Ne and Ar is not healed. Only
Schrader's model and the present model, in which the
correlation effects are treated via the atomic polarizabili-
ty, give the correct decreasing trend when going from Ne
to Xe. Schrader's model seems to give band gaps which
are too narrow by a nearly constant factor. The correla-
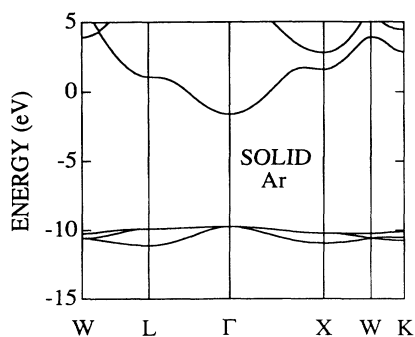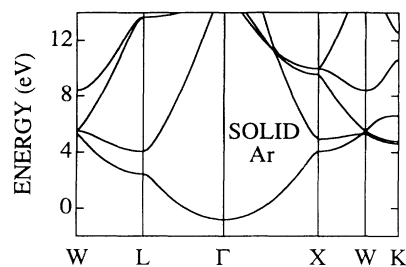tion potential of Eq. (5) gives nearly perfect agreement.

FIG. 3. The positron band structure for solid Ar.

The results for the band gap E_g^+ were found relatively in-
sensitive to the parameter r_1. The choice $r_1 = 1.7$ a.u. for
all rare-gas solids gives the band gap within the experi-
mental uncertainties as shown in Table I. The depen-
dence near $r_1 = 1.7$ a.u. is nearly linear with the deriva-
tive dE_g^+/dr_1 around 0.3 eV (a.u.)$^{-1}$.

The other parameter that can be extracted from the
measurements by Gullikson, Mills, and McRae[6] is the
positron work function. In order to compare it with
theory one should determine the position of the bottom
of the positron bands relative to the vacuum. The
present bulk calculations performed in the ASA give the
positron and electron energy levels relative to the same
well-defined reference level, the crystal zero.[12,13] The
crystal zero is defined in the present case by the fact that
the Coulomb potential vanishes on the surface of the neu-
tral atomic sphere.

The energy-level scheme for electrons and positrons is
shown in Fig. 5. The vertical energy scale corresponds to
the results for Ar. The bottom of the positron bands
(ε_0^+) is below the crystal zero (CZ) and the difference,
defined as a negative quantity, is the positron chemical
potential (μ_+). The distance from the bottom of the posi-
tron bands to the vacuum level is the positron work func-
tion $(\phi_+ > 0)$. In the case of electrons the bottom (ε_c) of
the conduction bands is slightly below the crystal zero.
The top of the valence bands (ε_v) is lower by the large en-
ergy gap. The distance from the crystal zero to the top of
the valence band defines the electron chemical potential

FIG. 2. The scalar relativistic electron band structure for
solid Ar.

TABLE II. Properties of electron bands in rare-gas solids.
E_g is the band gap between the valence and conduction bands in
the LDA and according to experiments (expt) (Ref. 20). E_v is
the measured distance between the valence band and the vacu-
um level (Ref. 21). ΔE_{SIC} is the self-interaction correction cal-
culated for the uppermost occupied energy level in a free atom.
μ_- is the self-interaction-corrected electron chemical potential,
i.e., $\mu_- = \mu_-(LDA) + \Delta E(SIC)$. All energies are in eV.

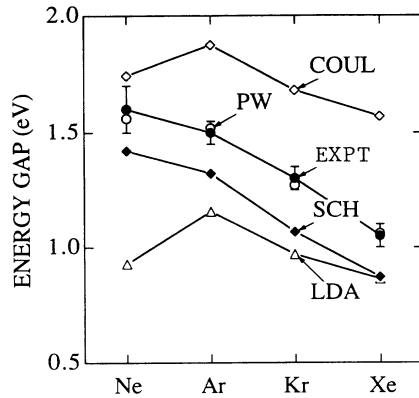| Host	E_g(LDA)	E_g(expt)	E_v	ΔE_{SIC}	μ_-
Ne	11.46	21.69	20.3	−9.37	−22.64
Ar	8.14	14.15	13.8	−5.36	−15.11
Kr	6.73	11.60	11.9	−4.55	−13.30
Xe	5.73	9.28	9.8	−3.78	−11.37

FIG. 4. Positron band gap E_g^+ at the L point of the Brillouin zone. The results obtained in different models for the positron correlation potential are compared with the measured values (Ref. 6).
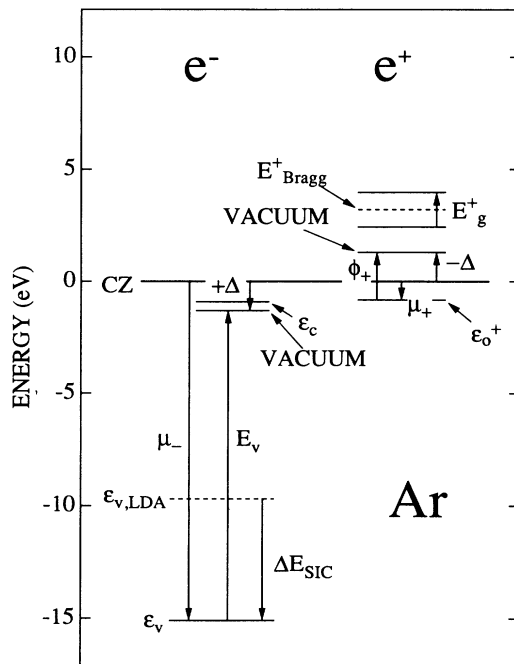

FIG. 5. Electron and positron energy levels and their differences in a rare-gas solid. The vertical scale corresponds to Ar in the present model and the energy zero is the crystal zero (CZ) discussed in the text. ε_c and ε_v are the bottom of the conduction bands and the top of the valence bands for electrons, respectively. $\varepsilon_{v,\mathrm{LDA}}$ is the pure LDA result for the top of the valence bands. ε_0^+ is the bottom of the positron bands. E_{Bragg}^+ and E_g^+ are, respectively, the position and width of the first-order Bragg peak at the L point of the Brillouin zone of the positron band structure (see Fig. 3). Δ is the dipole potential step at the surface. μ_- and μ_+ are the electron and positron chemical potentials, respectively. ϕ_+ is the positron work function, E_v the distance from the top of the electron valence bands to vacuum, and ΔE_{SIC} is the self-interaction correction for the valence bands. Arrows pointing upwards and downwards denote positive and negative quantities, respectively.

(μ_-), and the distance from the top of the valence band to the vacuum level (E_v) corresponds to the electron work function. Both for positrons and electrons the vacuum level is separated from the crystal zero by the dipole potential step (Δ). Because this energy is of electrostatic origin the steps for electrons and positrons are the same in magnitude but opposite in direction. In order to determine the positron work function we calculate the dipole potential step from the theoretical electron chemical potential and the measured[21] distance between the top of the valence band and the vacuum level. Thus,

$$\phi_+ = -\mu_+ - \Delta = -\mu_+ - \mu_- - E_v \ . \tag{6}$$

There is a problem in the determination of the theoretical values for the electron chemical potential. Namely, although the density-functional method itself will give the position of the uppermost occupied electron level correctly, the self-interaction effects inherent in the LDA can shift it considerably upwards.[5] While this is not the case for metals where the Fermi-level electrons are free to move over the whole solid, self-interaction effects are expected to be prominent in the LDA description of rare-gas solids with narrow valence-electron bands. We have estimated the shift of the electron chemical potential by calculating the uppermost p-electron energy levels of the rare-gas atoms both in the LDA and in the corresponding self-interaction-correction method (SIC).[9] The results for this correction ΔE_{SIC} and the values of the ensuing electron chemical potential as well as the values of the experimental positions of the top of the valence-electron band with respect to the vacuum level are given in Table II. The SIC correction is important. It amounts up to 40% of the total magnitude of the electron chemical potentials, which are now much more negative than the electron chemical potentials for metals [they are typically between 0 and -2 eV (Ref. 13)].

As already noted by Perdew and Zunger[9] the SIC corrections calculated for free atoms estimate very well the correction needed for the LDA band gaps of the rare-gas solids. This is because the SIC correction for the relatively well-localized valence states in the solid is expected to be similar to those for the uppermost free-atom states whereas there should be no SIC correction for the delocalized conduction states. This notation supports our correction to the electron chemical potential.

The positron chemical potentials and the "theoretical" positron work functions obtained in different models for the positron correlation potential are given in Table III. The experimental positron work functions are also shown for comparison. All theoretical work functions are larger than the experimental ones. The proposed model [Eq. (5)] for the positron correlation potential gives values closest to the measured work functions. The largest discrepancy, 1.4 eV, is in the case of Ne. However, one should bear in mind that the value of the positron work function results in this case from a near cancellation of terms in magnitude of about 20 eV, so that errors in different approximations such as the SIC correction (about 9 eV in magnitude) or the omission of the spin-orbit splitting may have an important contribution. Both

TABLE III. Positron properties for rare-gas solids. μ_+, ϕ_+, and A_+ are the positron chemical potential, the work function, and the positron affinity, respectively. They are calculated using the present (PW), LDA, and Schrader's (SCH) positron correlation potential. The experimental (expt) positron work functions (Ref. 6) are given for comparison. All energies are in eV.

Host	μ_+(PW)	ϕ_+(PW)	A_+(PW)	μ_+(LDA)	ϕ_+(LDA)	μ_+(SCH)	ϕ_+(SCH)	ϕ_+(expt)
Ne	+0.35	1.99	−22.29	−5.62	7.95	−0.39	2.73	0.6±0.1
Ar	−0.82	2.13	−15.93	−5.20	6.51	−2.00	3.32	1.55±0.05
Kr	−1.25	2.65	−14.55	−5.17	6.57	−2.38	3.77	2.00±0.05
Xe	−1.83	3.40	−13.20	−5.03	6.59	−3.01	4.57	2.30±0.05

the present and Schrader's model reproduce well the experimental increasing trend in the positron work function when going from Ne to Xe. On the contrary, the LDA values decrease from Ne to Ar and thereafter the positron work function is nearly constant.

The electron affinity is defined as the distance from the electron vacuum level to the bottom of the conduction band. Because for Ar and Ne the former is below the latter the electron affinity is negative. For Kr and Xe the electron affinity is positive. We have defined in Ref. 13 the *positron* affinity A_+ as the sum of the electron and positron chemical potentials

$$A_+ = \mu_- + \mu_+ . \tag{7}$$

For metals and metal alloys the positron affinity difference between two materials, e.g., a precipitate and the host alloy matrix, in contact with each other gives directly an effective potential-energy difference between these materials. For insulators with large band gaps the situation is, however, more complicated because one should know the actual position of the electron chemical potential, or the Fermi level, in the band gap. Thus one cannot use it directly, e.g., to discuss the trapping of positrons into solid rare-gas bubbles in metals.[22] Anyway, we have given in Table III for completeness the resulting values of the positron affinity using the top of the valence band for the electron chemical potential. The positron affinities are now large negative numbers because of the

electron contribution. For comparison, the positron affinities for metals and semiconductors are between −1 and −8 eV.[13] For these materials the lowest values result mainly from the low positron chemical potentials.

IV. CONCLUSIONS

We have made a theoretical analysis of the positron reemission results for rare-gas solids by Gullikson, Mills, and McRae.[6] We introduce for rare-gas solids a semi-empirical positron correlation potential which depends only on the polarizability of the atom in question. The experimental results for the positron energy band gap at the L point of the Brillouin zone and for the positron work function can be systematically explained if the positron correlation and the electron exchange-correlation effects are taken into account beyond the local-density approximation. The width of the positron band gap reflects directly the properties of the positron potential. The positron work function is a more indirect measure because we have to use in its determination the measured electron work functions and a self-interaction correction term calculated for free atoms. We present a systematic analysis of the absolute positions of the energy levels.

[1]For a review, see P. J. Schultz and K. G. Lynn, Rev. Mod. Phys. **60**, 701 (1988).

[2]E. M. Gullikson and A. P. Mills, Jr., Phys. Rev. Lett. **57**, 376 (1986).

[3]A. P. Mills, Jr. and E. M. Gullikson, Appl. Phys. Lett. **49**, 1121 (1986).

[4]M. Tuomisaari, R. H. Howell, and T. McMullen, J. Phys. B **24**, 1455 (1991).

[5]For a recent review, see R. O. Jones and O. Gunnarsson, Rev. Mod. Phys. **61**, 689 (1989).

[6]E. M. Gullikson, A. P. Mills, Jr., and E. G. McRae, Phys. Rev. B **37**, 588 (1988).

[7]For a review, see *Rare Gas Solids*, edited by M. L. Klein and J. A. Venables (Academic, London, 1976), Vols. 1 and 2.

[8]D. M. Ceperley and B. J. Alder, Phys. Rev. Lett. **45**, 566 (1980); we use their local exchange-correlation functional as parametrized in Ref. 9.

[9]J. Perdew and A. Zunger, Phys. Rev. B **23**, 5048 (1981).

[10]For a review, see O. K. Andersen, O. Jepsen, and M. Sob, in *Electronic Band Structure and Its Applications*, edited by M. Yussouff (Springer-Verlag, Heidelberg, 1987), p. 1.

[11]J. Arponen and E. Pajanne, Ann. Phys. (N.Y.) **121**, 343 (1979); J. Phys. F **9**, 2359 (1979).

[12]O. V. Boev, M. J. Puska, and R. M. Nieminen, Phys. Rev. B **36**, 7786 (1987).

[13]M. J. Puska, P. Lanki, and R. M. Nieminen, J. Phys. Condens. Matter **1**, 6081 (1989).

[14]M. J. Puska, S. Mäkinen, M. Manninen, and R. M. Nieminen, Phys. Rev. B **39**, 7666 (1989).

[15]D. M. Schrader, Phys. Rev. B **20**, 918 (1979).

[16]I. V. Abarenkov and I. M. Antonova, Phys. Status Solidi B **64**, 747 (1974).

[17]See Yan Li, J. B. Krieger, M. R. Norman, and G. J. Iafrate, Phys. Rev. B **44**, 10437 (1991), and references therein.

[18]See C. Kittel, *Introduction to Solid State Physics* (Wiley, New York, 1976).

[19]T. M. Miller and B. Bederson, Adv. At. Mol. Phys. **13**, 1 (1978); R. R. Teachout and R. T. Pack, At. Data **3**, 195 (1971).

[20]R. Haensel *et al.*, Phys. Rev. Lett. **23**, 116 (1969); **25**, 1281 (1970); Opt. Commun. **2**, 59 (1970).

[21]N. Schwentner *et al.*, Phys. Rev. Lett. **34**, 528 (1974).

[22]For a review, see R. M. Nieminen in *Proceedings of the VIII International Conference on Positron Annihilation,* edited by L. Dorikens-Vanpraet, M. Dorikens, and D. Segers (World Scientific, Singapore, 1989), p. 60.